

## High Levels of Winter Air Pollution under the Influence of the Urban Heat Island along the Shore of Tokyo Bay

HIROSHI YOSHIKADO

*National Institute for Resources and Environment, Tsukuba, Ibaraki, Japan*

MAKOTO TSUCHIDA\*

*Tsukuba University Graduate School, Tsukuba, Ibaraki, Japan*

(Manuscript received 20 November 1995, in final form 4 March 1996)

### ABSTRACT

A wintertime small-scale sea breeze associated with high levels of air pollution is described, in which the urban heat island plays an important role.

Over a major portion of the Kanto plain, the winter surface air temperature varies diurnally, ranging from 0° to 12°C on average. The water temperature in the innermost part of Tokyo Bay, surrounded by the plain, is maintained at 8°–10°C. The land–sea temperature contrast that generates sea breezes, however, is intensified by two processes: (i) the heat island associated with the Tokyo metropolitan area on the northwestern shore of the bay increases the land air temperature, and (ii) the nocturnal outflow of cool land air, the result of radiative cooling, covers the bay, causing the sea air temperature to be lower than the water temperature during the morning hours. As a result, the sea breeze frequently penetrates into the heavily urbanized area, extending about 20 km from the bayshore.

Since the sea breeze is coupled with the heat island, it does not penetrate farther inland. A convergence zone persists over the urbanized area, which in turn results in very high concentrations of pollutants.

An analysis of a typical episode is also discussed to more realistically describe the behavior of air pollution than for the averaged case.

### 1. Introduction

High concentrations of air pollutants are very often associated with calm and stable conditions. In the case of the southern Kanto plain including the Tokyo metropolitan area of Japan, ambient air pollutants such as nitrogen dioxide (NO<sub>2</sub>) and suspended particulate matter (SPM) exceed the respective standard concentrations most frequently during the early winter.

In this region, a characteristic meteorological pattern related to the surrounding terrain was found to induce occasional episodes of very high pollutant concentrations (Mizuno and Kondo 1992; Yoshikado et al. 1994). This pattern is accompanied by a local stationary front across Tokyo Bay, to the north of which a frontal inversion covers the plain to a height of several hundred meters and calm conditions persist. In contrast,

to the south of the front, a synoptic-scale southwesterly wind prevails and the air quality is quite good.

Even without the local front, however, calm and stable conditions associated with severe air pollution events frequently form over the Kanto plain. The meso-scale structure proves to be similar to the cold air lake generally observed in basins.

With any pattern, under such weather conditions as low wind speeds and clear skies, sea-breeze-like weak winds having 1-day cycles appear with high probability on the shore of Tokyo Bay in spite of the winter season, and in turn influence the pollution concentrations. The sea water temperature in Tokyo Bay, however, is not low enough in the winter compared with the land air temperature to induce the sea breeze. Therefore, the mechanism and detailed behavior of the winter sea breeze are of special interest, but they have never been selected as the main subject of a detailed analysis.

Another source of interest is as follows. For typical thermal conditions during the summer in middle latitudes, Yoshikado (1990, 1992) demonstrated that the heat island of a large city such as Tokyo affects the sea-breeze pattern to a greater degree than expected. This result leads to the question of what effect the urban heat island exerts during the winter when the sea breeze is weaker and less active.

---

\* Current affiliation: Tokyo Electric Power Company, Chiyoda-ku, Tokyo, Japan.

---

Corresponding author address: Dr. Hiroshi Yoshikado, National Institute for Resources and Environment, 16-3 Onogawa, Tsukuba, Ibaraki 305, Japan.  
E-mail: yosikado@nire.go.jp

The heat island effect on the airflow under calm conditions has been discussed by several authors. For example, Shreffler (1979) reported convergence over the urban center of St. Louis, which is considered to be the lowest portion of the heat island circulations. Fujibe and Asai (1980) detected convergence over the city of Tokyo under an average of weak pressure gradient conditions, which might include factors other than the heat island effect. Even with these past investigations, the airflow pattern associated with the heat island and its role in pollutant transport has not been sufficiently analyzed.

It would also be useful to clarify the significance of the heat island during the winter from the viewpoint of air pollution based on observational data, for a better understanding of the actual environment, and for the evaluation of simulation models.

Presently, it has been observationally found that the photochemical production of  $\text{NO}_2$  was quite active, even during winter (Kaneyasu et al. 1993). Very high concentrations of SPM also occurred exclusively in the same season. The modeling of this kind of event is now under way, the results of which will be published in the near future. The accurate simulation of air pollution is based on a sufficient understanding of meteorological processes and their incorporation into the model. The present analysis is found to be indispensable in accomplishing this procedure.

## 2. Description of the area and data

The Tokyo metropolitan area is one of the largest and most highly populated cities in the world, located along the northwestern shore of Tokyo Bay (cf. see Fig. 4). The heavily urbanized area is almost completely covered by artificial materials and extends about 20 km or more from the shore. It is surrounded by the Kanto plain, the area of which is roughly  $100 \text{ km} \times 100 \text{ km}$ . On the north and west side of the plain, mountain ranges are found to heights of 2000 m.

During the summer, the sea breeze develops, not only over the plain, but over the mountainous region as a result of the coupling with upslope wind systems (Kondo 1990a,b; Kurita et al. 1985). In contrast, two meteorological conditions alternately appear during the winter. The cold northwesterly monsoon persists for one to several days, followed by a mild period. The events of current interest then occur (cf. Fig. 1); weak sea breezes are observed along the shore area at a high probability, accompanied by severe air pollution over the plain.

Since the concentrations of  $\text{NO}_2$  and SPM exceed their standard values most frequently during December over the Kanto plain area, the background of high-level air pollution is analyzed for the two Decembers of 1989 and 1990. Next, for the statistical analysis of the winter sea breeze, data for six months over the two winter seasons were processed: December 1989–February

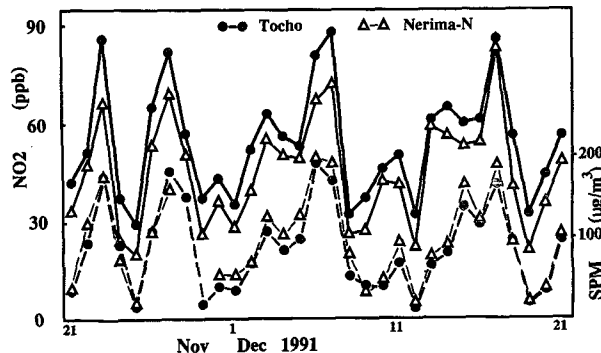


FIG. 1. An example of day-to-day variations of daily averaged concentrations of  $\text{NO}_2$  (solid lines) and SPM (broken lines) at selected stations in the Tokyo metropolitan area.

1990 and December 1990–February 1991. A typical episode, discussed below, was selected from December 1991.

For these analyses, hourly data from the two datasets were employed: pollutants, wind, and air temperature from the Air Quality Monitoring System (AQMS) in the Tokyo metropolitan area, and wind, air temperature, and sunshine duration from the Automated Meteorological Data Acquisition System (AMeDAS) sites located in the Kanto plain. The concentrations of pollutants and sunshine duration are averaged values for the prior 1 h, while the winds are averaged over the preceding 10 min. Temperatures are instantaneous values.

In addition, air temperature data at a midbay berth were available in the form of an analog chart. Roughly speaking, the accuracy of these temperatures was  $0.5^\circ\text{C}$ .

## 3. Background of high-level air pollution

### a. Distributions of daily averaged concentrations

To clarify the horizontal extent of the air pollution, correlations of the daily averaged concentrations among a number of AQMS stations were examined. Figure 2 shows the relationship of SPM concentrations between stations A and D (see Fig. 4 for station location). The former station is located in the inland part of the heavily urbanized Tokyo area, while the latter is found in a residential area about 38 km farther inland from A. The daily averaged value for A tends to be systematically larger than that for D, with a high correlation (correlation coefficient  $R = 0.92$ ).

The suburban station B is highly correlated with A ( $R = 0.97$ ) and D ( $R = 0.96$ ), whereas the correlation with the nearshore station C is somewhat lower ( $R = 0.90$ ). These relationships indicate that the SPM pollution has a very wide structure over the central area of the plain, with a timescale of 1 day or longer, although individual patterns of diurnal variation can somewhat differ from site to site.

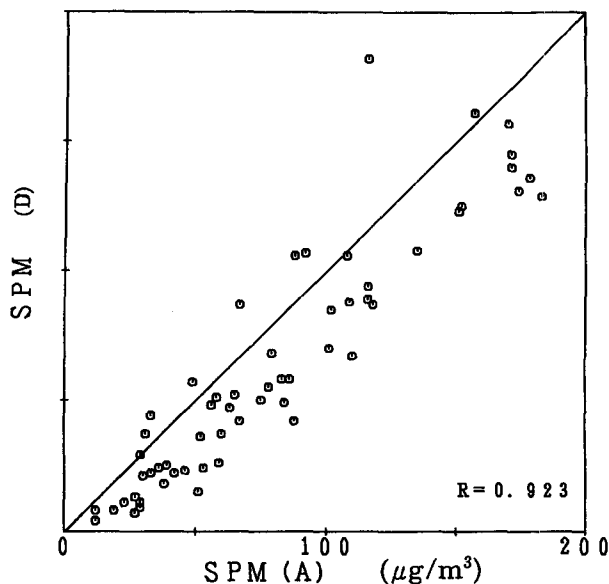


FIG. 2. Comparison of the daily averaged SPM concentrations at stations A and D during December 1989 and 1990. The locations of the stations are indicated in Fig. 4.

Furthermore, the behavior of  $\text{NO}_2$  pollution is basically similar to that of SPM, as can be seen in Fig. 1.

#### b. Air temperature and the daily averaged concentrations

According to a comparative analysis of aerological data, the AMeDAS site at the top of Mount Tsukuba (870 m above sea level), an isolated peak in the Kanto plain, gives a representative temperature of the upper atmosphere above the plain, although its location is several tens of kilometers from the region of present interest.

The vertical stability, evaluated as the temperature difference between Mount Tsukuba and Urawa, an AMeDAS site near B (Fig. 4), is positively correlated ( $R = 0.89$ ) with the SPM concentration, as shown in Fig. 3a.

Figure 3a also indicates that the wind direction is an important factor related to the levels of pollution. Several days of very high concentration are characterized by southwesterly winds, which appear above the frontal inversion associated with the local front mentioned in section 1. Below the frontal inversion, the air is stagnant, and high levels of pollutants are observed. The cases of high concentration without southwesterlies should occur during periods of strong surface inversions.

Most of the days with small concentrations are accompanied by winds from the northwest or north. These wind directions represent the winter monsoon, prevailing not only at the mountain level, but also at the surface of the plain.

Hereafter, the cases when the daily mean value of SPM is not less than  $130 \mu\text{g m}^{-3}$  are called high-SPM days, while those less than  $90 \mu\text{g m}^{-3}$  are termed low-SPM days. Values at B were selected as representative values. Figure 3a reveals that on the average, the temperature difference is estimated as  $5^\circ\text{C}$  higher on high-SPM days than on low-SPM days. In other words, the  $5^\circ\text{C}$  anomaly means that anomalous cooling is found at Urawa on high-SPM days.

Similarly, the temperature at any point on the surface of the plain can be examined as related to Urawa. For example, from Fig. 3b the temperature anomaly at Maebashi on high-SPM days is estimated as  $2.4^\circ\text{C}$ . Figure 4 shows the distribution of this temperature anomaly. The broad area with small values means that on high-SPM days the temperature decreases in this area simultaneously with that at Urawa.

The central area with small anomalies is surrounded by mountains along which relatively high temperature anomalies are found, and the area appears as a cold air lake. The area is open only on the southeast side, where the Tokyo metropolitan area and Tokyo Bay appear to block the cold air. The large values of the anomaly, or warming, on the southeast side of the "cold air lake" are associated with two factors. One is the warm southwesterly wind to the south of the local front previously mentioned. The other factor is the urban heat island over Tokyo and the warm sea surface, which can dominate under calm conditions. In the following, the thermal structure of the latter is examined through an analysis of the winter sea breeze.

## 4. Characteristics of the winter sea breeze

### a. Screening of sea-breeze days

#### 1) SELECTION OF CLEAR CALM DAYS

The number of sample days examined was 180, six months of the two winters. Eighty-six days were selected as appropriate for sea-breeze development due to weak pressure gradients and relatively strong insolation. Hereafter, "calm" means that the synoptic pressure gradients are weak.

The criteria for the pressure gradient were taken from the corresponding geostrophic wind speeds  $V_g$ . First, the  $V_g$  evaluated from the sea level pressures of six observatories located in central Japan over a 200-km-scale area must be less than  $15 \text{ m s}^{-1}$ . Second, the  $V_g$  evaluated by five observatories in the Kanto plain on a scale of 100 km must be less than  $7.5 \text{ m s}^{-1}$ . These criteria were based on Fujibe (1981), except that the threshold values had to be modified for winter weather conditions, when the pressure patterns tend to vary over shorter periods than in summer.

On the other hand, the insolation data were evaluated by the sunshine duration SS at one AMeDAS station in Tokyo, since the weather in the plain did not differ greatly from place to place. The criterion for clear days

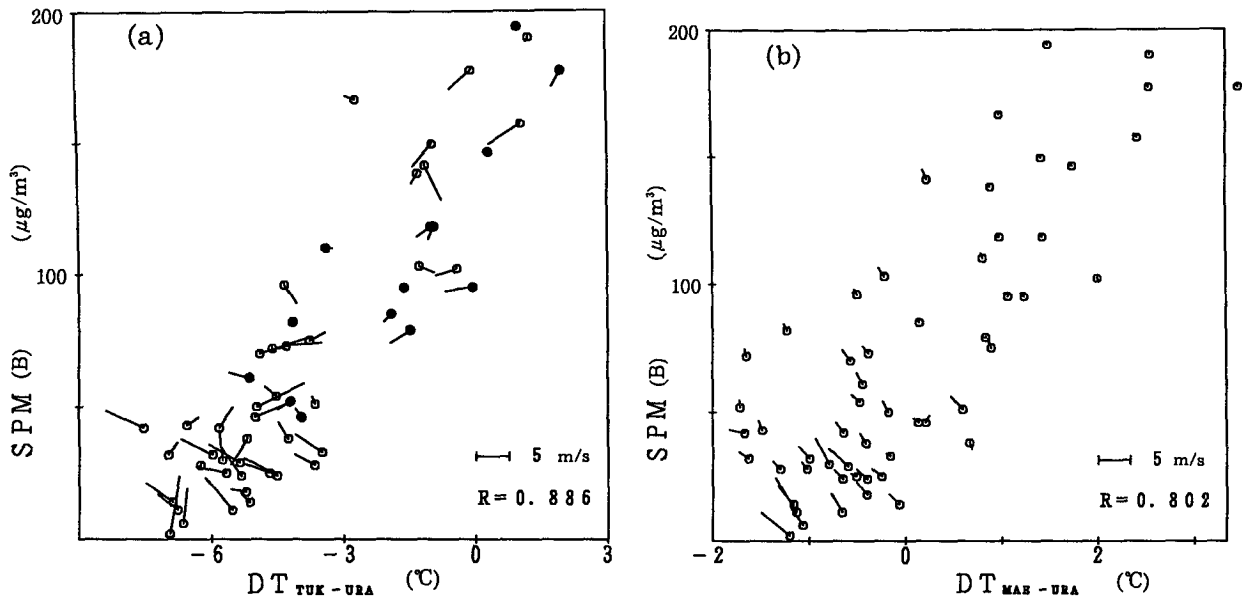


FIG. 3. (a) The daily averaged SPM concentration at B as a function of the daily averaged temperature difference between Mount Tsukuba and Urawa (near B). The averaged wind speed and direction at Mount Tsukuba are indicated by the small bars, where an upward bar represents a north wind. The samples represented by solid circles indicate the sea-breeze days mentioned in section 4. (b) Same as in (a) except that the abscissa represents the temperature difference between Maebashi (northwest corner of the plain) and Urawa, and the small bars indicate the wind at Urawa.

was determined as the average SS between 0900 and 1500 Japan standard time (JST) being greater than 0.5. Namely, the duration of sunshine totaled at least 3 h during the 6-h period.

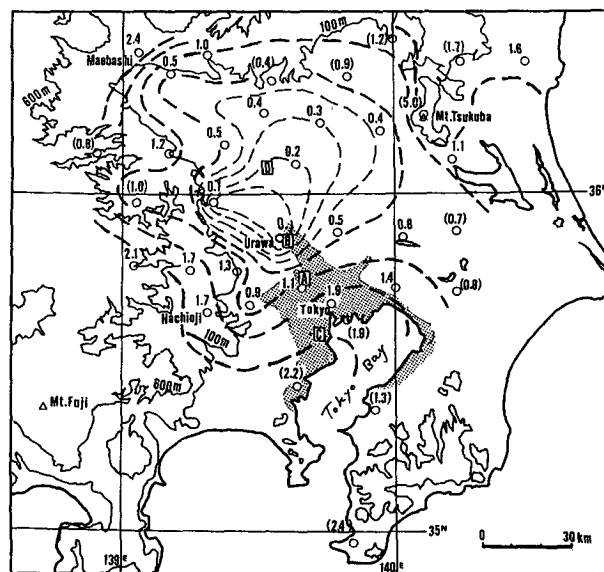


FIG. 4. Distribution of averaged anomaly  $DT_H - DT_L$  ( $^{\circ}\text{C}$ ), where  $DT_H$  and  $DT_L$  are the temperature differences at each point from Urawa on high-SPM days (daily average  $> 130 \mu\text{g m}^{-3}$ ) and on low-SPM days (daily average  $< 90 \mu\text{g m}^{-3}$ ), respectively. The numerals in parentheses denote  $\text{rms}(DT_H)$  or  $\text{rms}(DT_L) > 1.0^{\circ}\text{C}$ . The stippled area represents the heavily urbanized area of Tokyo.

## 2) SELECTION OF SEA-BREEZE DAYS

Sea-breeze days were selected from the clear calm days, judging from the diurnal variation of the wind direction at two nearshore sites, indicated as 1 and 5 in Fig. 5a. Three conditions were set that had to be satisfied simultaneously at both sites. That is, (i) the wind direction for the sea breeze was defined as southeasterly ranging from east to south-southwest, (ii) this wind direction had to be first observed during 0800–1800 JST and persist for at least three consecutive hours, and (iii) the sea-breeze direction should terminate before 2300 JST or later were excluded, since such persistent winter sea breezes probably resulted from external forcing. Overall, 41 days were selected as sea-breeze days.

### b. Thermal structure responsible for inducing the sea breeze

The averaged temperature distribution for the sea-breeze days (Fig. 5b) is quite important to understand the mechanism of the breeze, when taking into consideration that the local winds such as land and sea breezes generally flow from cooler to warmer areas.

At 0600 JST, the air temperature is near  $0^{\circ}\text{C}$  over the inland area and about  $6^{\circ}\text{C}$  above the bay. Under these conditions, a land breeze is expected to develop, although a slightly adverse gradient exists near the shore. The sea air temperature of  $6^{\circ}\text{C}$  is less than the water temperature, which is usually  $8^{\circ}\text{--}10^{\circ}\text{C}$  during

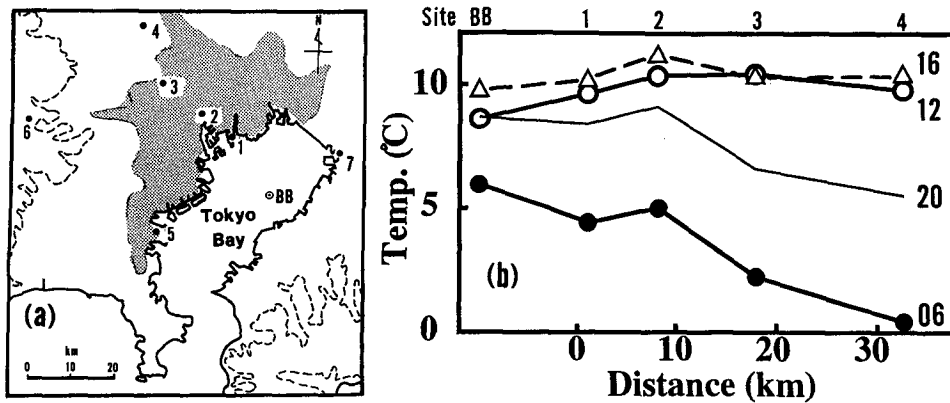


FIG. 5. (a) The AMeDAS sites referred to in section 4 (solid circles) and the midbay berth (BB). Dotted lines are the contours of 100 m ASL. (b) Horizontal distributions of surface air temperature. The distance is measured northwestward from the bayshore to Urawa (site 4). The numerals on the right-hand side are hours in JST.

winter in this area of the sea (e.g., Shimoyama 1977). This cold air is considered to result from advection associated with the land breeze. The land breeze is actually observed as northerly or northwesterly, as will be shown later.

After 0600 JST, the sea air reaches the same temperature as the sea water. The inland area is also heated, but attains a daily maximum only slightly higher than the sea air temperature. This land–sea temperature contrast appears to be insufficient to induce a sea breeze. In reality, the urban heat island along the shore intensifies the land–sea temperature contrast to about 2°C. This value is quite small compared with the summer temperature contrast, resulting from temperatures of 26°–27°C above the sea and 30°–35°C above the plain in the afternoon.

At the same time, the urban heat island maintains a temperature gradient down to the inland area. Thus, the urban heat island tends to reinforce the sea breeze in the shore area, and to prevent it from penetrating through the urban region. Such a sea breeze as this may be more suitably characterized as the “heat island circulation.”

After 1600 JST, the inland temperature decreases rapidly, and a temperature gradient appropriate for the land breeze is again intensified. The land–sea temperature contrast is not clear due to the urban heat island maintaining the shore area as warm as the sea air, so that the land breeze is actually not a suitable term. The probable extension of the drainage flow from the mountainous region may be a major factor in this circulation.

### c. Behavior of the sea breeze

#### 1) DIURNAL VARIATION OF WINDS

As shown in Fig. 6, the southeasterly sea breeze is observed from 1200 to 1800 JST at the nearshore site 1

(cf. Fig. 5a for the location). The maximum wind speed of 2.9 m s<sup>-1</sup> occurs at 1500 JST. At site 2, about 8 km from the shore, the sea breeze appears from 1300 to 1800 JST, with a maximum of 1.6 m s<sup>-1</sup> at 1600 JST.

In farther-inland areas, however, the southeasterly component is hardly detected and the variation in wind direction is slight. Site 3, on the inland side of the Tokyo urban center and 18 km from the shore (the wind hodograph is not shown), and site 4 located in the suburbs 33 km from the shore, are typical of the inland areas. These results reflect the fact that the sea breeze does not necessarily reach these sites, even on what are considered sea-breeze days, or the sea breeze is very weak in the event that it does reach the sites.

On the other hand, at sites near the mountainous region, such as site 6, clear changes in wind direction are found, suggesting the development of valley and mountain wind.

At 1500 JST, around which time the sea breeze attains maximum speed (Fig. 6), the representative wind direction of the sea breeze—that is, southeast—prevails over the urbanized region of Tokyo as a whole (Fig. 7). In closer detail, however, the wind speed is notably weak in the northwest section of the metropolitan area and becomes stronger again in areas farther west. These are consistent with the description of the diurnal wind variations.

#### 2) DURATION OF THE SEA BREEZE

To further clarify the behavior of the sea breeze, its onset and cessation times were examined for sites 1, 3, and 4. The sea-breeze direction was determined as east to south-southwest, the same as in section 4a.2(i), for all the sites. The onset at any site is defined as the time when the sea-breeze direction is first observed after and including 0800 JST. The cessation time is then defined

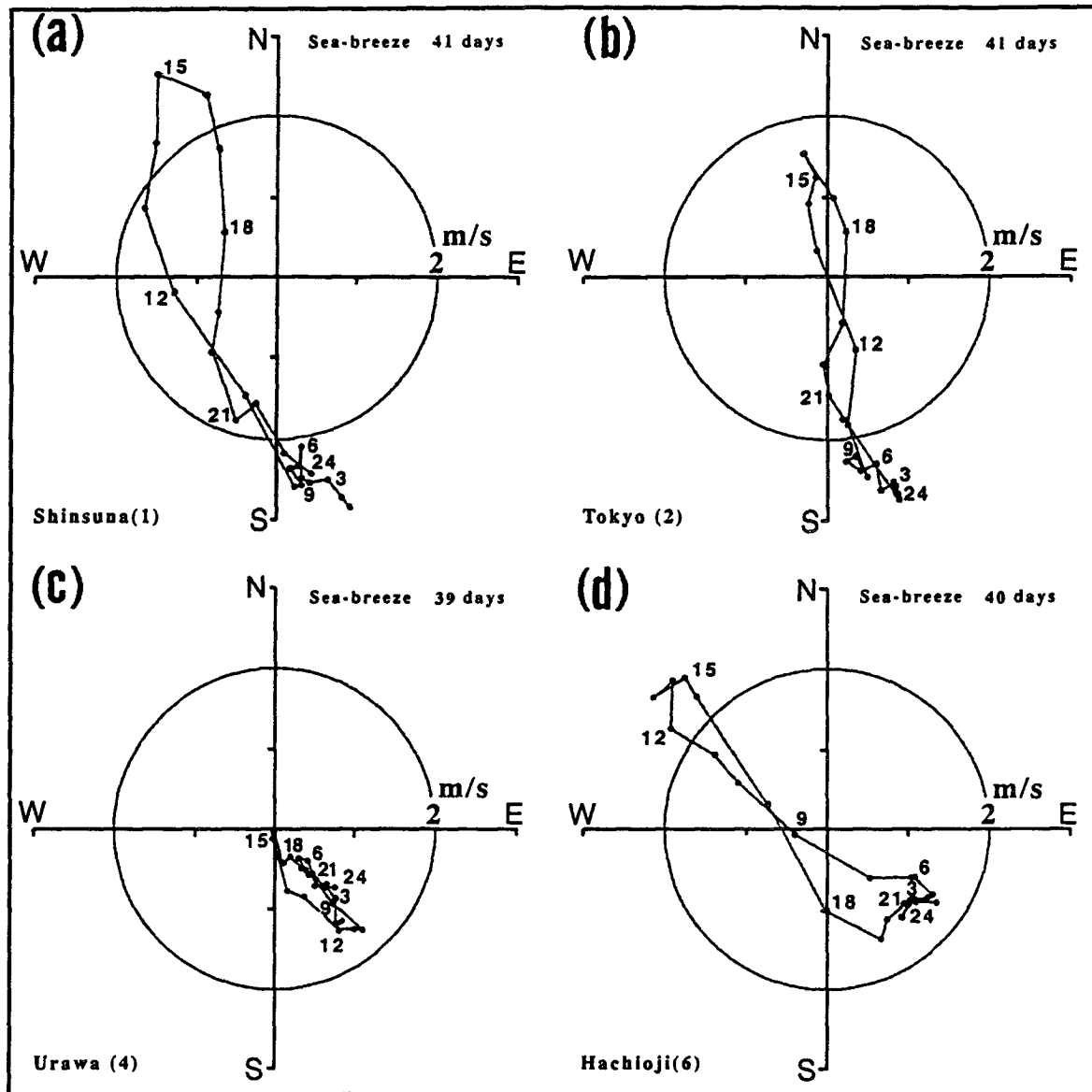


FIG. 6. Diurnal wind variations averaged for the sea-breeze days at sites (a) 1, (b) 2, (c) 4, and (d) 6 as shown in Fig. 5a. Each point with respect to the origin indicates the wind vector head at the given time (hours in JST).

as when any wind direction other than that of the sea breeze is first observed after the onset. In addition, even if the sea breeze direction appeared at sites 3 and 4 at an earlier time than at site 1, and did not persist until the onset at site 1, it was not categorized as a sea breeze.

The averaged results are listed in Table 1. On the average for site 1, the onset occurs between 1200 and 1300 JST, while it varies from 1000 to 1600 JST. The averaged cessation time is between 1900 and 2000 JST, varying from 1600 to 2300 JST. Since the distributions of the onset and cessation times are nearly split, it is easily determined that the sea breeze occurs most prob-

ably between 1500 and 1600 JST at site 1. The duration of the sea breeze averages 6.6 h, but it is scattered over 3–11 h, with 3 h found as the minimum duration [in section 4a(2ii)].

The variability in the period of occurrence mentioned above suggests that the winter sea breeze is very sensitive to the winds or pressure systems on scales larger than the phenomenon. This suggestion is associated with two facts. One is that the winter sea breeze generally occurs on a smaller scale compared with that in warm seasons. The other fact is that the pressure patterns are changeable during the winter, even during the mild periods.

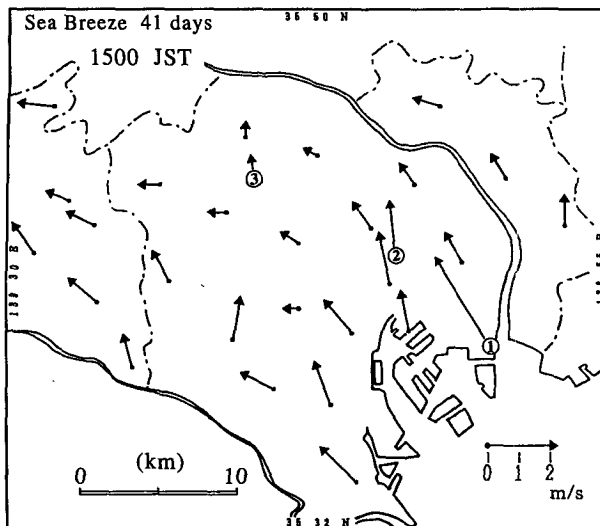


FIG. 7. Wind vectors at 1500 JST averaged for the sea-breeze days. Data from the AQMS were used. The area surrounded by the dash-dotted lines is the Tokyo metropolitan area. The circled numerals indicate the AMeDAS sites corresponding to Fig. 5a.

The sea breeze appeared at site 3 on 34 days and at site 4 on 28 days of the 41 sea-breeze days. Although the criterion for the duration of sea-breeze direction of only 1 h was used at these sites, if this criterion was changed to 2 h, the number of days decrease to 23 and 16 days, respectively. Furthermore, although the duration at site 4 is 3.1 h, as listed in Table 1, such cases when the sea-breeze direction actually persisted for no less than 3 h occurred on only 6 days. For these six particular days, the duration of the sea breeze averaged 9.2 h at site 1, 6.5 h at site 3, and 4.3 h at site 4. Namely, when the duration of the sea breeze is long in the near-shore area, it tends to also persist for long periods in inland areas. The duration at site 4 is, however, shorter than half of that at site 1 even in this case.

Some consideration given to the speed of the sea breeze as it extends inland may be meaningful. It is improper to calculate the speed simply based on Table 1. For the 34 days when the sea breeze reaches site 3, the averaged onset time at site 1 is 1224 JST, and the extending speed between sites 1 and 3 is evaluated as  $14 \text{ km h}^{-1}$ . A similar calculation results in a somewhat larger value for the section between sites 3 and 4. These are unexpectedly large when the speed of the sea breeze

and the land-sea temperature contrast mentioned above are taken into consideration; the maximum speed of the sea breeze found in Fig. 6a is  $2.9 \text{ m s}^{-1}$ , or  $10.4 \text{ km h}^{-1}$ . If the temperature and pressure are horizontally uniform over the land, such that the sea breeze is induced only by the land-sea temperature contrast, the sea breeze must have definite characteristics of a gravity current. In this case the extending speed of the current head never exceeds the speed of the current (cf. Simpson 1994). Therefore, for the case of the winter sea breeze reaching the inland side of the Tokyo urban center, it is probably influenced, or even induced, by a thermal structure similar to that which induces the valley wind. In other words, the sea breeze tends to prevail only at the shore side of the urban center but appears to advance inland when the valley wind system is simultaneously well developed. Under summer conditions, these two wind systems form into one extended local wind system that further develops. During the winter, however, even if they are connected at around 1500 JST, the wind speeds decrease rapidly after that time, as shown in Fig. 6.

### 3) COMPARISON WITH THE OPPOSITE SHORE

The thermal structure mentioned in section 4b suggests that the heat island over Tokyo is an important factor in inducing the winter sea breeze. To examine what would happen in the absence of the heat island effect, the sea breeze over the eastern shore of Tokyo Bay was analyzed. There, the population is smaller than 10% of that in the western shore, and, thus, the eastern shore represents a situation with less heat island effect.

On the eastern shore of Tokyo Bay, the sea breeze generally backs, from westerly to southerly, in response to the distribution of topography there. Therefore, along the eastern shore, the first condition that the sea breeze should satisfy [section 4a.2(i) for the west shore sea breeze] was modified as follows: (i) At site 7 (Fig. 5a), the wind direction of the sea breeze was defined as southwesterly, ranging from south to west. The conditions (ii) and (iii) remained the same as those defined previously for the western shore.

From a total of 86 clear calm days, 32 days were selected as satisfying the sea-breeze criteria for the eastern shore, which is clearly less than 41 sea-breeze days observed for the Tokyo area. A total of 25 days satisfied the sea-breeze criteria for both western and eastern shores.

TABLE 1. Averaged duration of the sea breeze.

Site (number of days)	Distance from the shore (km)	Onset time (A) (JST)	Cessation time (B) (JST)	Duration (B - A) (h)
1 (41)	1	1248	1924	6.6
3 (34)	18	1336	1736	4.0
4 (28)	33	1418	1724	3.1

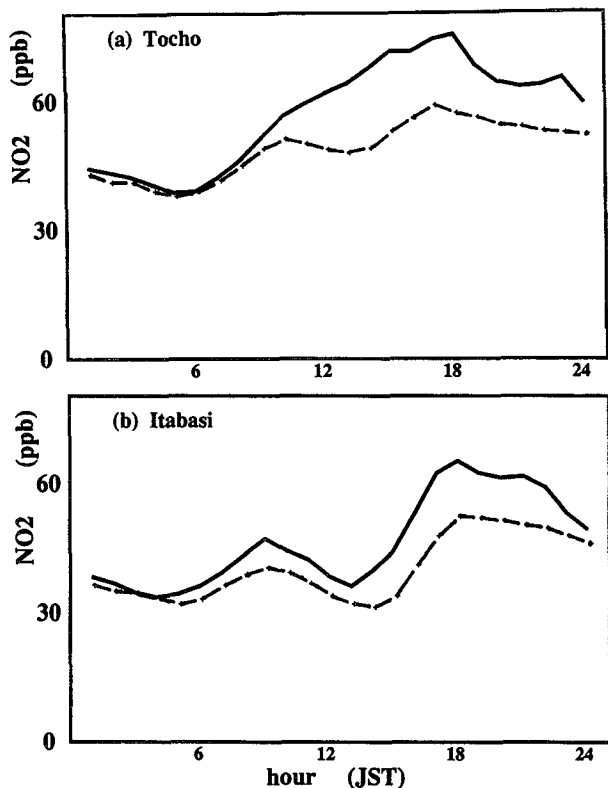


FIG. 8. Diurnal variations of NO<sub>2</sub> concentration averaged for the sea-breeze days (bold lines) and clear calm days with no sea breeze (dashed lines) at (a) a AQMS station near site 2 and (b) near site 3.

The wind speed at site 7, averaged for the east shore sea-breeze days, attains a maximum value of 2.75 m s<sup>-1</sup> from the west-southwest at 1500 JST. This value is comparable to the maximum value of 2.9 m s<sup>-1</sup> observed at site 1.

d. Behavior of air pollutants

1) AVERAGED DIURNAL VARIATION

As was shown in Fig. 1, the variations in the patterns of NO<sub>2</sub> and SPM are basically similar. Therefore, only the behavior of NO<sub>2</sub> will be discussed below.

Generally the NO<sub>2</sub> concentration has two daily peaks. One occurs during the morning hours, while the maximum is observed during the evening. These peaks mainly occur in proportion to the traffic density, and due to the formation of a stable layer, especially in the evening. This is true for the Tokyo metropolitan area, where the two peaks are found in most cases (Fig. 8b). In the shore area, however, the pattern differs on winter sea-breeze days (Fig. 8a). Namely, the decrease does not occur in the early afternoon, around which time the sea breeze is most prevalent in the shore area. This suggests that the sea air contains high concentrations of pollutants. It is inferred that the pollutants are trans-

ported, either by the land breeze that prevails over the shore until the onset of the sea breeze or by the upper-level offshore flow above the sea breeze.

Figure 8 also indicates that concentrations are higher on sea-breeze days than those found on other clear calm days. Whereas light winds tend to remove the pollutants, even on calm days, the circulation system may capture the pollutants on sea-breeze days. This inference is considerably confirmed by the following case study.

2) CASE STUDY

An intensive field observation was performed during 6 and 7 December 1991 to clarify the detailed process of high-level air pollution over the southern Kanto plain, when severe pollution was actually observed (cf. Fig. 1). The behavior of the sea breeze and that of the pollutants during this period were not only consistent with the above analysis but were quite suggestive in clarifying the mechanism and role of the winter sea breeze.

On 6 December the sea breeze was initiated at 1100 JST over the southmost shore area of Tokyo and extended to the area of the southeast half of Tokyo during 1200 through 1500 JST (Fig. 9). After that time, the sea breeze retreated from the land, and a northerly land breeze prevailed all over the area after 1700 JST. Throughout the duration of the sea breeze, the most highly polluted area occurred at the frontal zone between the land and sea breezes.

On 7 December the sea breeze was first observed at 1300 JST at the nearshore sites, and advanced mainly northward until 1600 JST. Simultaneously, a landward

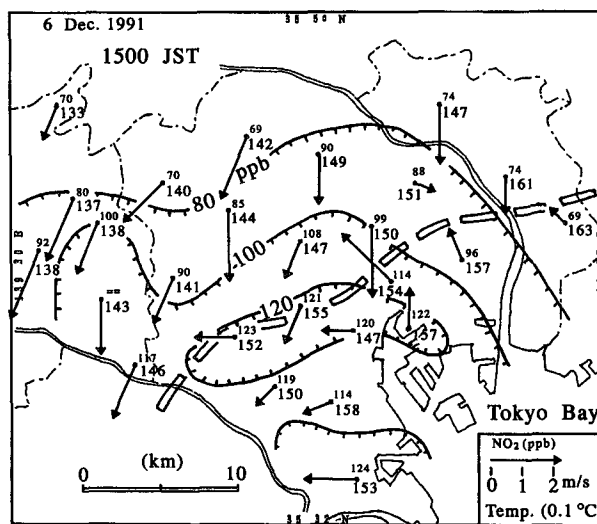


FIG. 9. Horizontal distributions of surface wind, temperature, and NO<sub>2</sub> concentration (ppb) in the Tokyo area at 1500 JST 6 December 1991. The data are from AQMS stations. The sea-breeze front is indicated by the open-blocked line.



local wind system extended from the west (Fig. 10), and appeared to connect with the sea breeze during the evening. However, a westerly land breeze appeared over the western portion of the area at 1900 JST, and prevailed over Tokyo at 2000 JST. In Fig. 10, a zone of seaward breezes was found to remain over the inland half of the Tokyo area. In this zone, ozone ( $O_3$ ) concentrations increased to around 40 ppb, whereas the sea-breeze area having concentrations of  $O_3 < 10$  ppb extended to this zone by 1700 JST. This increase in ozone presumably resulted from the vertical exchange of air, accompanied by the divergence between the seaward breeze and the westward inland wind.

The differences in the distributions of  $NO_2$  between Figs. 9 and 10 indicate that there are two types of severe air pollution induced by the winter sea breeze. One type occurs in the frontal zone of the sea breeze, which tends to remain over the urban center. On the other hand, the type such as that found on 7 December will probably occur on the second or a later day in the series of sea-breeze days. This results from the formation of a highly polluted air mass during the prior day or night, accumulating over the bay before the onset of the sea breeze. Such a polluted air mass could be the result of a sea breeze being developed the day before.

## 5. Conclusions

In the present paper, the thermal conditions in the Kanto plain were first analyzed, being associated with very high levels of pollutants often observed in early winter. Based on daily averages, a cold air lake was found to cover the central part of the plain. The process of formation of this cold air mass has recently been analyzed with use of a three-dimensional numerical model (Kondo 1995).

Pollutant sources, including mobile sources, are widely distributed over the plain, so that the calm and stable conditions that accompany the cold air lake result in severe air pollution over a large part of the plain. It should be noted here that the cold air lake is not blocked by the mountainous regions, but on the southeast side only by the large urban area of Tokyo. Two meteorological phenomena are related to the high temperatures in the southeast region of the plain and the severe pollution. One is the mesoscale stationary front with a warm southwesterly wind on the southeast side, and the other is the urban heat island accompanied by the winter sea breeze.

The sea breeze occurs on about 20% of the days during the 3 months of winter. The land-sea temperature contrast that results in the sea breeze is, on the average, as follows. The sea air temperature is at about  $6^\circ\text{C}$  during the early morning as a result of the nocturnal land breeze inflow, whereas it becomes equivalent to the bay water temperature of  $8^\circ\text{--}10^\circ\text{C}$  by noontime. On the other hand, the land air temperature increases to about  $12^\circ\text{C}$  in the urban area along the shore, with

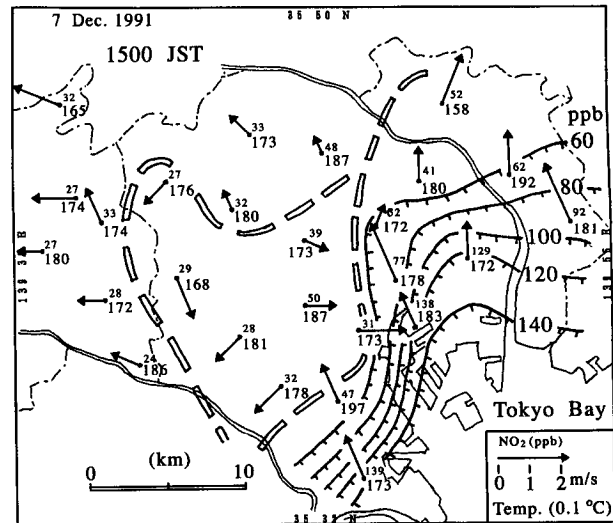


FIG. 10. Same as in Fig. 9 except for 7 December 1991.

the inland air temperature being lower. Therefore, the winter sea breeze possesses a characteristic of the heat island circulation; it does not frequently advance inland through the urban center, and a convergence zone tends to remain over the urban center for several hours.

Consistent with the behavior of the sea breeze, higher concentrations of air pollutants than those in the inland stagnant area remain over the urban area for a long period of time. Occasionally, pollutants accumulated over the bay during the previous night are added to these concentrations. Furthermore, the sea breeze does not develop as it does in summer, but presumably forms a closed circulation system above the shore area, preventing the diffusion of urban pollutants.

An inland local wind system similar to the valley wind often develops over the inland areas of the plain during the afternoon. The domain of this system may become connected with the sea-breeze area in their mature stage. They soon begin to decay, however, without developing as an extended system.

*Acknowledgments.* The authors wish to express their thanks to Professor Emeritus T. Kawamura of the University of Tsukuba for constant encouragement and advice. They are indebted to Dr. M. Kobayashi, Dr. R. Suzuki, and Prof. T. Yasunari of the university for helpful discussions. A considerable part of the present study was performed in preparation for the master thesis of M. Tsuchida, submitted to the university. The AQMS data were provided by the authorities of the Tokyo and Saitama Prefectural Office.

## REFERENCES

- Fujibe, F., 1981: Seasonal characteristics of land and sea breezes (in Japanese). *Tenki*, **28**, 367–375.

- , and T. Asai, 1980: Some features of a surface wind system associated with the Tokyo heat island. *J. Meteor. Soc. Japan*, **58**, 149–152.
- Kaneyasu, N., H. Yoshikado, T. Mizuno, T. Tanaka, K. Sakamoto, Q.-Y. Wang, and M. Sofuku, 1993: Photochemical products measured in early-winter severe air pollution episodes in the Tokyo Metropolitan Area, Japan. *Proc. Int. Spec. Conf. Regional Photochemical Measurement and Modeling Studies*, San Diego, CA, Air & Waste Management Association, 345–351.
- Kondo, H., 1990a: A numerical experiment of the “extended sea breeze” over the Kanto Plain. *J. Meteor. Soc. Japan*, **68**, 419–434.
- , 1990b: A numerical experiment on the interaction between sea breeze and valley wind to generate the so-called “extended sea breeze.” *J. Meteor. Soc. Japan*, **68**, 435–446.
- , 1995: The thermally induced local wind and surface inversion over the Kanto plain on calm winter nights. *J. Appl. Meteor.*, **34**, 1439–1448.
- Kurita, H., K. Sasaki, H. Muroga, H. Ueda, and S. Wakamatsu, 1985: Long-range transport of air pollution under light gradient wind conditions. *J. Climate Appl. Meteor.*, **24**, 425–434.
- Mizuno, T., and H. Kondo, 1992: Generation of a local front and high levels of air pollution on the Kanto Plain in early winter. *Atmos. Environ.*, **26A**, 143–154.
- Shimoyama, N., 1977: Sea surface temperature. Report of the special observation for atmospheric environment in the South Kanto Area I (in Japanese). Japan Meteor. Agency Rep. 90-92, 241 pp. [Available from Japan Meteor. Agency, 1-3-4 Ohtemachi, Tokyo, Japan.]
- Shreffler, J. H., 1979: Heat island convergence in St. Louis during calm periods. *J. Appl. Meteor.*, **18**, 1512–1520.
- Simpson, J. E., 1994: *Sea Breeze and Local Wind*. Cambridge University Press, 234 pp.
- Yoshikado, H., 1990: Vertical structure of the sea breeze penetrating through a large urban complex. *J. Appl. Meteor.*, **29**, 878–891.
- , 1992: Numerical study of the daytime urban effect and its interaction with the sea breeze. *J. Appl. Meteor.*, **31**, 1146–1164.
- , T. Mizuno, and S. Shimogata, 1994: Observed structure of terrain-induced air stagnation over the southern Kanto Plain in early winter. *Bound.-Layer Meteor.*, **68**, 159–172.